Research Square

Preprints are preliminary reports that have not undergone peer review.
They should not be considered conclusive, used to inform clinical practice,
or referenced by the media as validated information.

Preparation of hybrid coal gangue-polyacrylamide adsorbent and analysis of its performance for removal of Cu2+ and Pb2+ from wastewater

Shanshan Sun
ji ning yi xue yuan: Jining Medical University
Zhu ZHU
ji ning yi xue yuan: Jining Medical University
Shujie Wang
ji ning yi xue yuan: Jining Medical University
Yongdong ZHANG
Jining Medical College: Jining Medical University
Huiyun WANG
Jining Medical University
Xiangao Quan (quanxg3696@163.com)
Jining Medical College: Jining Medical University

Research Article

Keywords: hybrid adsorbent, coal gangue, acrylamide, graphite furnace atomic absorption spectroscopy

Posted Date: March 9th, 2021

DOI: https://doi.org/10.21203/rs.3.rs-290887/v1

License: This work is licensed under a Creative Commons Attribution 4.0 International License.
Read Full License

Preparation of hybrid coal gangue-polyacrylamide adsorbent and analysis of its performance for removal of Cu^{2+} and Pb^{2+} from wastewater

Shanshan SUN Zhu ZHU Shujie WANG Yongdong ZHANG Huiyun WANG Xiangao QUAN *

Shanshan SUN (330628104@qq.com), Zhu ZHU (737007550@qq.com), Shujie WANG (350637829@qq.com),Yongdong ZHANG (58989937@qq.com), Huiyun WANG (wang_huiyun@126.com), Xiangao QUAN* (quanxg3696@163.com)

School of Pharmaceutical Science, Jining Medical University, Shandong 276826, China

* Corresponding author: Xiangao QUAN

Abstract: This study describes the preparation of a low-cost adsorbent (hybrid coal gangue–polyacrylamide (HCGPAM)) based on activated coal gangue and acrylamide, and explores the effects of using it to remove Cu^{2+} and Pb^{2+} from wastewater. It investigated factors such as the impact of the initial concentrations of Pb^{2+} and Cu^{2+}, adsorption time and temperature, and solution pH. The HCGPAM was fully characterized using Fourier transform infrared spectrometry, scanning electron microscopy, X-ray diffraction, and atomic absorption spectrometry (AAS), and the Pb^{2+} and Cu^{2+} concentrations were measured using graphite furnace AAS. The adsorption performance experiment was conducted at 25 ℃ with initial Pb^{2+} and Cu^{2+} concentrations of 100 $ug \cdot ml^{-1}$, an adsorbent dosage of 0.350 g, and an adsorption time of 30 min. The pH values of the Pb^{2+} and Cu^{2+} solutions were 5 and 4, respectively. When the adsorption effect was at an optimum, the Pb^{2+} and Cu^{2+} attained adsorption rates of 59.05% and 80.6%, respectively. The HCGPAM can be used to treat polluted sewage and therefore has favorable prospects for commercial application.

Highlights

- Hybrid coal gangue-polyacrylamide (HCGPAM) adsorbs Pb^{2+} and Cu^{2+} very effectively
- At its optimum, HCGPAM adsorbed 59.05% and 80.6% of Pb^{2+} and Cu^{2+}, respectively
- HCGPAM has a high potential for commercial application

Keywords: hybrid adsorbent; coal gangue; acrylamide; graphite furnace atomic absorption spectroscopy

1 INTRODUCTION

As global industrial activity increases rapidly, heavy metal pollution in aquatic environments is a serious concern for environmentalists due to the high toxicity and persistence of the pollutants. Heavy metal ions cannot be broken down to yield non-toxic species in the natural environment. Pb^{2+} and Cu^{2+} are commonly used in many industrial activities and two of the most toxic heavy metal ions found in water sources (Imasuen and Egai, 2013).

To date, techniques such as adsorption, flocculation, coagulation, membrane filtration, electrochemical operations, solvent extraction, and biosorption have been studied to effectively eliminate hazardous heavy metals from aqueous solution (Roosta et al., 2014; Jamshidi et al., 2015a; Jamshidi et al., 2015b). Some of these methods are costly and inefficient for use as ways to control heavy metal ion levels in wastewater. The primary disadvantage of the adsorption process is the high cost of the adsorbent, which increases the price of the wastewater treatment (Pawar et al., 2016). Adsorption techniques have unique advantages over other methods due to their simple design, use of low-cost, non-toxic materials, and their high efficiency in removing pollutants at low concentrations. Furthermore, the use of naturally abundant materials as adsorbents offers treatment technology that is also environmentally friendly.

Coal gangue (CG), a by-product of coal mining or coal washing, has become the most prominent solid waste of the coal industry and is produced in increasing amounts every year with the expansion of the coal industry (Jabłońska et al., 2017; Guo et al., 2016). CG is rich in valuable minerals such as SiO2, Al2O3, Fe2O3, and CaO (Yang et al., 2012). However, it adversely affects the natural landscape and leads to disasters including landslides and debris flows. A more serious effect is of CG is catacausis, which releases poisonous gases that heavily pollute the environment. Despite these problems, CG may be a valuable entity as its high iron content makes it suitable for use as a polyaluminium ferric silicate (PSFA) flocculant. Some researchers have attempted to prepare inorganic flocculants based on CG (Zhou et al., 2015, Chuncai et al., 2014; Cao et al., 2016; Wang et al., 2011). It was found that

calcination and subsequent alkali and acid leaching of the solid waste lead to a marked increase in its specific surface area, thus making it a potential raw material for organic-inorganic hybrid flocculants (Gao et al., 2015; Zhang et al., 2015).

In this study, a new CG–polyacrylamide (HCGPAM) adsorbent was synthesized by the in situ polymerization of an inorganic flocculant/AM (acrylamide) mixture. It was characterized by Fourier transform infrared spectrometry (FTIR), scanning electron microscopy (SEM), X-ray diffraction (XRD), and atomic absorption spectrometry (AAS). It has been used as a flocculant for oilfield drilling wastewater (Quan and Wang, 2014), but has not been studied as an adsorbent to remove metal ions from wastewater. HCGPAM can effectively adsorb Pb2+ and Cu2+ from wastewater and hence can be applied to treating sewage including Pb2+ and Cu2+; this has favorable market prospects. This study used graphite furnace atomic absorption spectrometry to explore the effects of utilizing HCGPAM as an adsorbent to remove Cu2+ and Pb2+ from wastewater (Glatstein and Francisca, 2015; Huang et al., 2015; Liu et al., 2014).

2 MATERIALS AND METHODS

2.1 Materials

The CG used in this study was obtained from a coal mine (Yanzhou mining bureau, China), and it was composed of 26.58% SiO_2, 5.35% Al_2O_3, 14.38% Fe_2O_3, 3.56% CaO, and 1.26% MgO. Polyacrylamide (PAM) was purchased from a water treatment plant (Henan Gongyi, China). All the chemical reagents were of analytical grade and supplied by Shanghai Chemistry Reagent Co. KBr was of spectrum pure reagent and supplied by Aladdin Reagent Co. Ltd. Standard Pb^{2+} and Cu^{2+} solutions (1000 μg/mL) were supplied by the State Center for Standard Matter. Water distilled using a Quartz Second Boiling High Pure Water Distiller was used to prepare all the solutions.

An AA-6800 atomic absorption spectrometer (Shimadzu, Japan), IRTracer-100 FTIR spectrometer (Shimadzu, Japan), a JSM-6700F scanning electron microscope (Japan Electronics), an INCA Energy X-ray diffractometer (Oxford instruments, United Kingdom), a TP213 electronic scale (Sartorius), a pHS-3C pH acidity meter

(Kangyi Corporation, Shanghai, China), and a 101 vacuum drying oven (Xianke Corporation, Longkou, China) were used in the experiments.

2.2 Methods

2.2.1 Preparation of HCGPAM

The CG was crushed into powder and sieved through a 100-mesh screen; the particles used in the experiment were smaller than 150 μm. Then it was calcined in a muffle furnace at 750 ℃ for 2 h. After cooling to 25 ℃, the CG was subjected to alkali leaching with 15% NaOH and acid leaching with 15% HCl at 100 ℃ and 5 MPa, and finally dried at 100 ℃.

Then 8 g of acrylamide (AM) and 90 ml of distilled water were added to a 250 ml polymerization bottle. After this, 3 g of modified CG powder was added to the solution, which was stirred for 30 min. The solution was vacuumized and purged with N_2 three times to completely remove oxygen, and then different amounts of the initiator $(NH_4)_2Ce(NO_3)_6$ were slowly injected into the polymerization bottle. The bottle was kept in a thermostated water bath at 70 ℃ (± 0.5℃) for 6 h. The solution in the polymerization bottle was transferred to a 250 ml beaker, precipitated with acetone, and kept immersed in acetone for 12 h. It was finally dried in a vacuum oven at 35 ℃ for 24 h.

2.2.2 Preparation of Pb^{2+} and Cu^{2+} stock solution

Accurate measurements of 3.3000 g lead nitrate and 6.0000 g copper nitrate were taken and then 100 mL of 3 M nitric acid solution was added to dissolve these salts. The solution was then diluted to 1000 mL with distilled water.

2.2.3 Preparation of the standard curve

Standard Pb^{2+} and Cu^{2+} standard solutions (100 $\mu g.ml^{-1}$) in 0.0, 0.20, 0.40 0.60,

0.80, and 1.00 mL quantities were transferred to 10 mL volumetric flasks and diluted with 0.3 M HNO_3 solution to prepare 0, 2, 4, 6, 8,10 μg mL^{-1} solutions, respectively. The absorbance of the Pb^{2+} and Cu^{2+} standard solutions was measured using graphite furnace atomic absorption spectrometry. The standard curve with absorbance as the ordinate and the concentration as the abscissa was drawn to obtain the linear regression equations below:

$$A=0.0908C+0.0087,\ R^2=0.9996\ (Pb^{2+}) \quad (1)$$

$$A=0.0576C-0.0032,\ R^2=0.9994\ (Cu^{2+}) \quad (2)$$

2.2.4 Absorption experiments on Pb^{2+} and Cu^{2+}

Then 200 mL of 100 μg mL^{-1} Pb^{2+} or Cu^{2+} solution was pipetted into a 500 mL beaker, after which 0.400 g HCGPAM was added. The pH of the Pb^{2+} and Cu^{2+} solutions was adjusted to 5 and 4 and the solutions were then stirred for 30 min at 25 °C. The solution was centrifuged at the rate of 3500 rpm for 20 min, before 1.00 mL of the supernatant was transferred to a 100 mL volumetric flask and diluted with 0.3 M HNO_3 to the mark. The absorbance was measured for different concentrations of Pb^{2+} and Cu^{2+} with distilled water as blank. The absorption rate η (%) was calculated according to formula (3) below:

$$\eta = \frac{C_0 - C_e}{C_0} \times 100\% \quad (3)$$

where C_0 is the concentration of Pb^{2+} or Cu^{2+} (μg mL^{-1}) before absorption and Ce is the concentration of Pb^{2+} or Cu^{2+} (μg mL^{-1}) after absorption.

2.2.5 Langmuir isotherms

Different concentrations of Pb^{2+} and Cu^{2+} solution 100 mL were transferred to a beaker and 1.0 g HCGPAM was added. The temperature of the water bath was adjusted to 23 °C. After adsorption for 2 h under constant stirring, the equilibrium concentrations of Pb^{2+} and Cu^{2+} were measured. The Langmuir isotherm equation (Formula 4) used for fitting the isothermal adsorption is as follows (He et al., 2013):

$$\frac{C_{eq}}{Q} = \frac{1}{K_L Q_{max}} + \frac{C_{eq}}{Q_{max}} \quad (4)$$

where C_{eq} is the adsorption equilibrium concentration (mol/L), Q is the equilibrium

adsorption quantity (mg/g), Q_{max} is the maximum equilibrium adsorption quantity (mg/g), and K_L is the adsorption equilibrium constant.

3 RESULTS AND DISCUSSION

3.1 FTIR, XRD, and SEM analyses

3.1.1 FTIR analysis

The FTIR spectra of HCGPAM adsorbent is illustrated in Figure 1. The absorption peaks at 3400 cm^{-1} and 3200 cm^{-1} attributing to N–H stretching bands and identified the presence of the free and aggregated $–NH_2$ bonds. The peak at 1650 cm^{-1} is assigned to N–H stretching vibration. The band at 800–1200 cm^{-1} is due to Si–O stretching vibrations and the peaks at 700 and 560 cm^{-1} are assigned to the bending vibrations of Si-O and Al-O. The peaks at 1140 cm^{-1} and 3000 cm^{-1} are assigned to C–O and C–H stretching vibrations, respectively. The band at 1400 cm^{-1} is attributed to the C–N stretching vibration, and the band at 1700 cm^{-1} is due to C=O stretching vibrations.

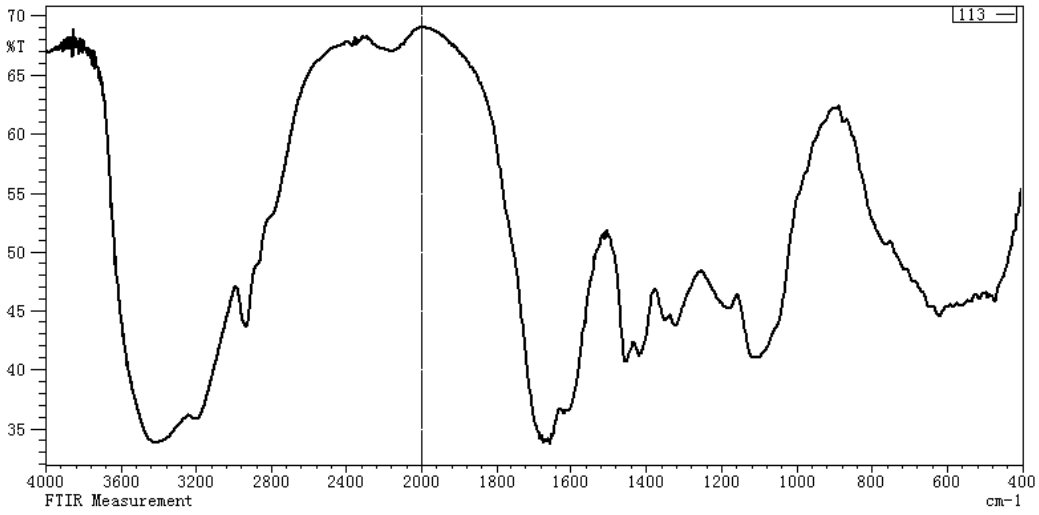

Fig. 1 FTIR spectrum of hybrid coal gangue–polyacrylamide

3.1.2 XRD analysis

The XRD patterns of the modified CG and HCGPAM are presented in Fig. 2 . Quartz patterns can be located at 20.82° ,21.34°(2 theta) in Fig. 2(a). It can be observed that the major mineralogical composition of the modified CG is quartz.This can be attributed to the reactions of the components (SiO_2, Al_2O_3, Fe_2O_3, CaO, and MgO) of CG with the acid and alkali used for leaching, which increased the relative amount and porosity of quartz remarkably(Quan and Wang, 2014). The diffraction

peaks according to Fig. 2(b) shows the presence of quartz and PAM. It reveals that the characteristic peaks caused by quartz decrease in intensity or disappear in the modified CG, whereas the characteristic peaks of PAM become more prominent. From the XRD patterns, it can be seen that PAM has entered the interlayer spacing of the CG.

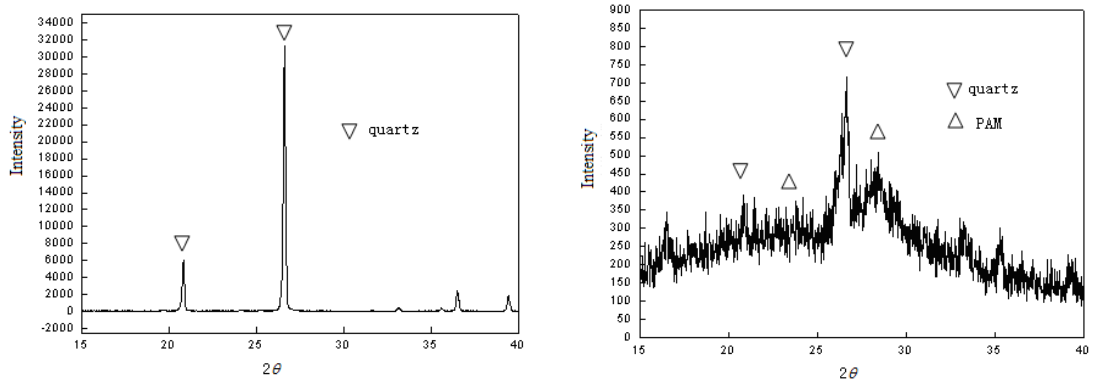

(a) Modified coal gangue **(b)** Hybrid coal gangue–polyacrylamide

Figure 2 XRD patterns of the samples

3.1.3 SEM analysis

The morphologies of the modified CG and HCGPAM were observed using SEM, and the results are presented in Fig. 3. HCGPAM has a surface morphology very different than that of the modified CG. The surface of HCGPAM resembles a cauliflower head, with a series of pleated ditches of different widths and depths, so that a coarser surface and larger specific surface areas than those of the modified CG are obtained.

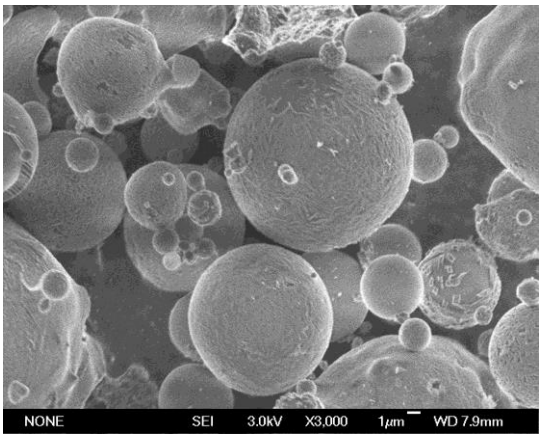

(a) Modified coal gangue

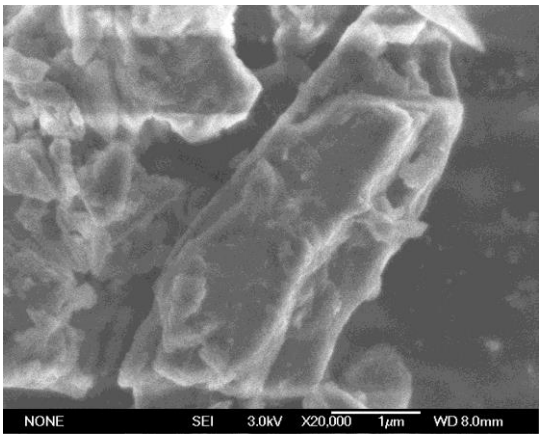

(b) Hybrid coal gangue–polyacrylamide

Figure 3 SEM images

3.2 Effect of adsorption conditions on adsorption properties of HCGPAM

3.2.1 Initial concentration of Pb^{2+} and Cu^{2+}

Pb^{2+} and Cu^{2+} solution (200 ml) with concentrations of 50, 100, 150, 200, 250, 300 $\mu g.ml^{-1}$ were prepared. and HCGPAM (0.3500 g) was added, stirred, and allowed to adsorb for 30 min at 25 ℃. The pH value of the solution was adjusted to 5 (Pb^{2+}) and 4 (Cu^{2+}). The absorption solution was centrifuged at 3500 rpm for 20 min; then 1.00 ml liquid supernatant was transferred into 100 ml volumetric flasks and diluted with 0.3 M HNO_3 to the mark. The absorbency was measured based on the different concentrations of Pb^{2+} and Cu^{2+}. Using formulas (1) and (2), the absorption rate (η, %) was calculated and the influence curve of the initial concentration of Pb^{2+} and Cu^{2+} were plotted with η as ordinate and the initial concentration of Pb^{2+} and Cu^{2+} as abscissa (Fig. 4).

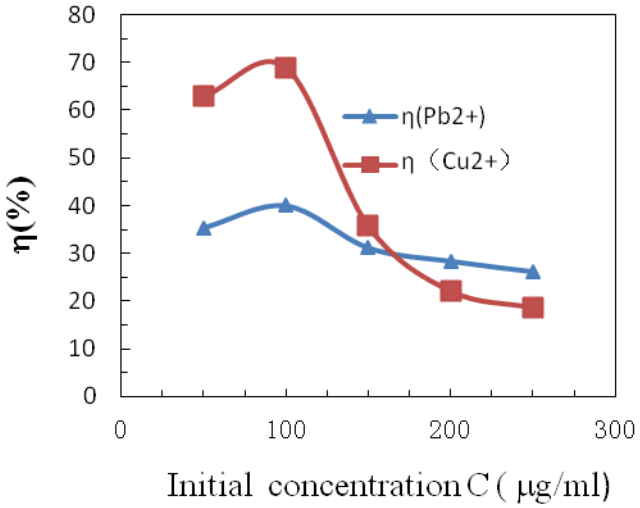

Fig. 4 Influencing curve for initial concentration of Pb^{2+} and Cu^{2+}

From Fig. 4, it can be seen that the adsorption rate (η) increases as the Pb^{2+} and Cu^{2+} concentration increases from 50 to 100 μg mL^{-}, but decreases with a further increase in the initial concentrations of these ions. The adsorptive sites are saturated with the increase in the initial concentration of Pb^{2+} and Cu^{2} so that the adsorption process becomes more competitive. Therefore, when the initial concentration of the ions is higher than 100 μg mL^{-1}, η decreases. Thus, we concluded that 100 $\mu g.ml^{-1}$ is the optimal initial concentration according to the experimental results.

3.2.2 Adsorbent dosage

Solutions of Pb^{2+} (100 $\mu g.ml^{-1}$) and Cu^{2+} (200 ml) were prepared and 0.250, 0.300, 0.350, 0.400, 0.450, 0.500 g HCGPAM were added, stirred, and adsorbed for 30 min at 25 °C. The pH of the solutions were adjusted to 5 (Pb^{2+}) and 4 (Cu^{2+}), they were centrifuged at 3500 rpm for 20 min, and then 1.00 ml liquid supernatant was transferred into 100 ml volumetric flasks and diluted with 0.3 M HNO_3 to the mark. Absorbency was measured based on different concentrations of Pb^{2+} and Cu^{2+}. Formulas (1) and (2) were used to calculate absorption rate (η, %) and the influence curve of HCGPAM dosage with η as ordinate and the HCGPAM dosage as abscissa was plotted (Fig. 5).

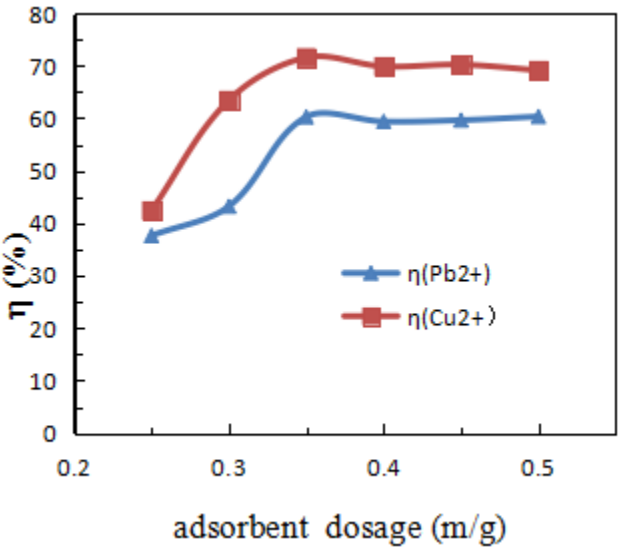

Fig. 5 Influence Curve of Adsorbent Dosage of Pb^{2+}, Cu^{2+}

From Fig. 5, it can be seen that the adsorption rate (η) of Pb^{2+} and Cu^{2+} rapidly increases from 0.25 g to 0.35 g as adsorbent dosage increases. However, with further increases in adsorbent dosage, η shows little change. This may be because the adsorption reaction reached absorption equilibrium. From the figure, it is clear that when the adsorbent dosage of Pb^{2+} and Cu^{2+} is 0.350 g, the best adsorption is achieved.

3.2.3 Adsorption Time

Solutions of 100 $\mu g.ml^{-1}$ Pb^{2+} and 200 ml Cu^{2} were prepared and 0.350 g HCGPAM were added. The solutions were stirred, and adsorption occurred for 10, 20, 30, 40, and 50 min at 25 ℃. The pH of the solutions were adjusted to 5 (Pb^{2+}) and 4 (Cu^{2+}), they were centrifuged at 3500 rpm for 20 min, and then 1.00 ml liquid supernatant was transferred into 100 ml volumetric flasks and diluted with 0.3 M HNO_3 to the mark. Absorbency was measured based on different concentrations of Pb^{2+} and Cu^{2+}. Formulas (1) and (2) were used to calculate absorption rate (η, %) and the influence curve of HCGPAM dosage with η as ordinate and the HCGPAM dosage as abscissa was plotted (Fig. 6).

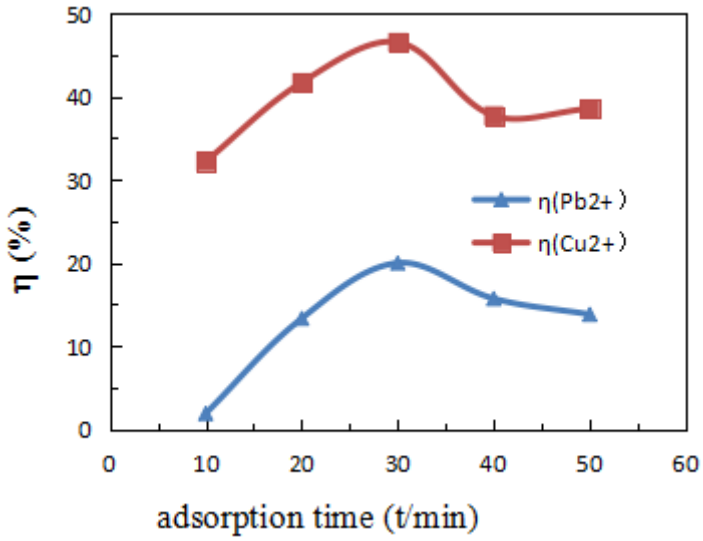

Fig. 6 Influence Curve of Adsorption Time of Pb^{2+}, Cu^{2+}

From Fig. 6, it can be seen that the adsorption rate (η) increased rapidly beginning at 30 min. Afterwards, when η is declined slightly, it might have been due to the absorption process being an ionic exchange reaction; the adsorption reaction likely reached the absorption equilibrium rapidly. Therefore, when the adsorption time of Pb^{2+} Cu^{2+} is 30 min, the adsorption effect is the best.

3.2.4 Adsorption Temperature

Pb^{2+} and Cu^{2+} solution (solution (100 μg.ml^{-1} and 200 ml, respectively) were prepared. HCGPAM (0.350 g) was added, stirred, and allowed to adsorb for 30 min at 25, 30, 35, 40, and 45°C, and the pH values of the solutions were adjusted to 5 (Pb^{2+}) and 4 (Cu^{2+}). The absorption solution was centrifuged at 3500 rpm for 20 min, then 1.00 ml liquid supernatant was transferred into 100 ml volumetric flasks and diluted with 0.3 M HNO_3 to the mark before absorbency was measured based on the different concentrations of Pb^{2+}, and Cu^{2+}.; Formula (1) and (2) were used to calculate absorption rate (η, %). The influence curve of adsorption temperature was plotted with η as ordinate and the adsorption temperature as abscissa (Fig. 7).

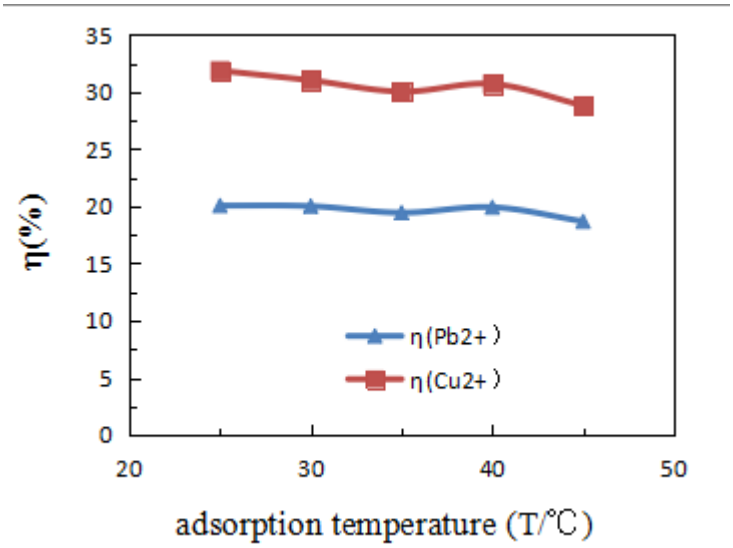

Fig. 7 Influence Curve of Adsorption Temperature of Pb^{2+}, Cu^{2+}

From Fig. 7, it can be seen that the adsorption rate (η) of Pb^{2+} and Cu^{2+} shows a small change as adsorption temperature increases. When the adsorption temperature of Pb^{2+} and Cu^{2+} is 25 ℃, the best adsorption effect is achieved.

3.2.5 Solution pH

Solutions of 100 μg.ml^{-1} Pb^{2+} and 200 ml Cu^{2} were prepared and 0.350 g HCGPAM were added. The solutions were stirred and allowed to adsorb for 30 min at 25 ℃, and the pH of the solution to was adjusted to 5 (Pb^{2+}) and 4 (Cu^{2+}). The absorption solution was centrifuged at 3500 rpm for 20 min before 1.00 ml liquid supernatant was transferred into 100 ml volumetric flasks and diluted with 0.3 M HNO_3 to the mark and absorbency was measured based on different concentrations of Pb^{2+} and Cu^{2+}. Formula (1) and (2) were used to calculate absorption rate (η, %). The influence curve of adsorption temperature was plotted with η as ordinate and the adsorption temperature as abscissa (Fig. 8).

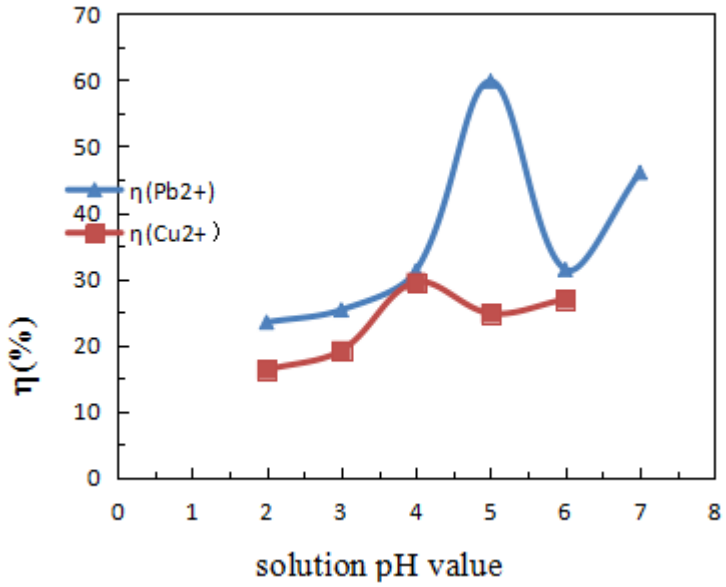

Fig. 8 Influence curve of the pH of the Pb^{2+} and Cu^{2+} solution

From Fig. 8, it can be seen that the adsorption rate (η) increased rapidly as pH increased from 2 to 5 (Pb^{2+}) and from 2 to 4 (Cu^{2+}). Subsequently, η showed a decreasing trend, but increased once again as pH exceeded 6 (Pb^{2+}) and 5 (Cu^{2+}). This may be because the product of the Pb^{2+} and Cu^{2+} solution began to precipitate. Thus, when the pH of Pb^{2+} and Cu^{2+} solution is 5 and 4, respectively, the best adsorption effect is achieved.

3.3 Langmuir Isotherm Curves

Figure 9 presents the Langmuir model fit for the adsorption of Pb^{2+} (Cu^{2+}) onto HCGPAM at 23 ℃. The Langmuir isotherm parameters of HCGPAM are shown in Table 1.

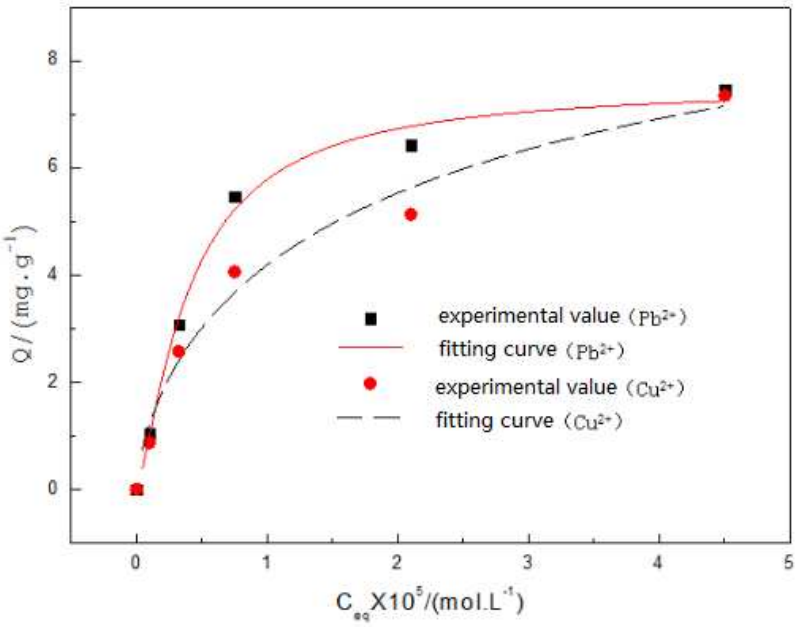

Fig. 9 Langmuir model fitting for the adsorption of Pb^{2+} (Cu^{2+}) onto hybrid coal gangue–polyacrylamide

Table 1 The Langmuir isotherm parameters for hybrid coal gangue–polyacrylamide

	Equation	Q_{max}/mg/g	K_L	R^2
Pb^{2+}	$C_{eq}/Q = 1.0483*10^{-6}+0.1138C_{eq}$	8.79	$1.0852*10^5$	0.95
Cu^{2+}	$C_{eq}/Q=7.4398*10^{-7}+0.0920C_{eq}$	10.87	$1.2365*10^5$	0.98

Table 1 shows the degree of fitting of Pb^{2+} (Cu^{2+}) is higher, indicating that the adsorption isotherm of HCGPAM to Pb^{2+} (Cu^{2+}) is in line with the Langmuir equation.

4 CONCLUSION

The absorption effect is optimal at an initial Pb^{2+} and Cu^{2+} concentration of 100 ug/ml and when the dosage of the adsorbent is 0.35 g, the adsorption time is 30 min, the temperature is 25 ℃ and the pH of the Pb^{2+} (Cu^{2+}) solution is 5 (4). Under these conditions, the Pb^{2+} and Cu^{2+} attain adsorption rates of 59.05% and 80.6%, respectively. The coal gangue-polyacrylamide hybridization adsorbent is very effective for Pb^{2+} and Cu^{2+}; therefore, it can be applied to treating sewage polluted with these elements, and market prospects for the commercial application of such a treatment is favorable.

Declarations

-Ethical Approval: Not applicable.

-Consent to Participate:Not applicable.

-Consent to Publish:Not applicable

-Authors Contributions: Zhu ZHU and Yongdong ZHANG preparated a low-cost adsorbent (HCGPAM), Huiyun WANG analyzed and interpreted the data regarding Langmuir Isotherm Curves. Shujie WANG and Shanshan SUN performed the adsorption examination , and was a major contributor in writing the manuscript. All authors read and approved the final manuscripShanshan

-Funding:This study was financially supported by Jining Medical College Support Fund(JYFC2018KJ017) and the National undergraduate innovation and entrepreneurship training program for local colleges and universities(201610443032, 201610443014，CX2016032) .

-Competing Interests: The authors declare that they have no competing interests.

-Availability of data and materials:All data generated or analysed during this study are included in this published article.

References

Cao, Z., Cao, Y., Dong, H., Zhang, J., Sun, C., 2016. Effect of calcination condition on the microstructure and pozzolanic activity of calcined coal gangue. Int. J. Miner. Process. 146, 23–28.

Chuncai, Z., Guijian, L., Dun, W., Ting, F., Ruwei, W., Xiang, F., 2014. Mobility behavior and environmental implications of trace elements associated with coal gangue: A case study at the Huainan Coalfield in China. Chemosphere. 95, 193–199.

Gao, Y., Huang, H., Tang W., Liu, X., Yang, X., Zhang J., 2015. Preparation and characterization of a novel porous silicate material from coal gangue. Microporous Mesoporous Mater. 217, 210–218.

Guo, Y., Yan, K., Cui, L., Cheng, F., 2016. Improved extraction of alumina from coal gangue by surface mechanically grinding modification. Powder Technol. 302, 33–41.

Glatstein, D.A., Francisca, F.M., 2015. Influence of pH and ionic strength on Cd, Cu and Pb removal from water by adsorption in Na-bentonite. Appl. Clay Sci. 118, 61–67.

He, J., Li, Y., Wang, C., Zhang, K., Lin, D., Kong, L., Liu, J., 2013. Rapid adsorption of Pb, Cu and Cd from aqueous solutions by β-cyclodextrin polymers. Appl. Surf. Sci. 426, Pages 29–39.

Huang, G., Wang, D., Ma, S., Chen, J., Jiang, L., Wang P., 2015. A new, low-cost adsorbent: Preparation, characterization, and adsorption behavior of Pb(II) and Cu(II). J. Colloid Interface Sci. 445, 294–302.

Imasuen, O.I., Egai, A.O., 2013. Concentration and environmental implication of heavy metals in surface water in Aguobiri Community, Southern Ijaw local government area, Bayelsa State, Nigeria. J. Appl. Sci. Environ. Manag. 17, 467–472.

Jabłońska, B., Kityk, A.V., Busch, M., Huber P., 2017. The structural and surface properties of natural and modified coal gangue. J. Environ. Manage. 190, 80–90.

Jamshidi, M., Ghaedi, M., Dashtian, K., Ghaedi, A.M., Hajati, S., Goudarzi, A., Alipanahpour, E., 2015a. Highly efficient simultaneous ultrasonic assisted adsorption of brilliant green and eosin B onto ZnS nanoparticles loaded activated carbon: Artificial neural network modeling and central composite design optimization. Spectrochim. Acta A Mol. Biomol. Spectrosc. 153, 257–67.

Jamshidi, M., Ghaedi, M., Dashtian, K., Hajati, S., Bazrafshan, A., 2015b. Ultrasound-assisted removal of Al3+ ions and Alizarin red S by activated carbon engrafted with Ag nanoparticles: central composite design and genetic algorithm optimization. RSC Adv. 5, 59522–32.

Liu, L., Li, Y., Liu, X., Zhou, Z., Ling, Y., 2014. Chelating stability of an amphoteric chelating polymer flocculant with Cu(II), Pb(II), Cd(II), and Ni(II). Spectrochim. Acta A Mol. Biomol. Spectrosc. 118, 765–775.

Pawar, R.R., Lalhmunsiama, Bajaj, H.C., Lee, S-M., 2016. Activated bentonite as a low-cost adsorbent for the removal of Cu(II) and Pb(II) from aqueous solutions: Batch and column studies. J. Ind. Eng. Chem. (Seoul, Repub. Korea) 34, 213–223.

Roosta, M., Ghaedi, M., Daneshfar, A., Sahraei, R., 2014. Experimental design based response surface methodology optimization of ultrasonic assisted adsorption of safaranin O by tin sulfide nanoparticle loaded on activated carbon. Spectrochim. Acta A Mol. Biomol. Spectrosc. 122, 223–31.

Quan, X.G., Wang, H.Y., 2014. Preparation of a Novel Coal Gangue–Polyacrylamide Hybrid Flocculant and Its Flocculation Performance. Chinese J. Chem. Eng. 22, 1055–1060.

Wang, H.Y., Quan, X.G., Shi, M.J., 2011. Preparation of coal gauge based PSFA and its application to the treatment of drilling wastewater. Ind. Water Treat. 31, 38–41.

Yang, M., Guo, Z., Deng, Y., Xing, X., Qiu, K., Long, J., Li, J., 2012. Preparation of $CaO–Al_2O_3–SiO_2$ glass ceramics from coal gangue. Int. J. Miner. Process. 102, 112–115.

Zhang, Y., Guo, Y., Cheng, F., Yan, K., Cao, Y., 2015. Investigation of combustion characteristics and kinetics of coal gangue with different feedstock properties by thermogravimetric analysis. Thermochim. Acta. 614, 137–148.

Zhou, C., Liu, G., Fang, T., Lam, P.K.S., 2015. Investigation on thermal and trace element characteristics during co-combustion biomass with coal gangue, Bioresource Technol. 175,454–462.

Figures

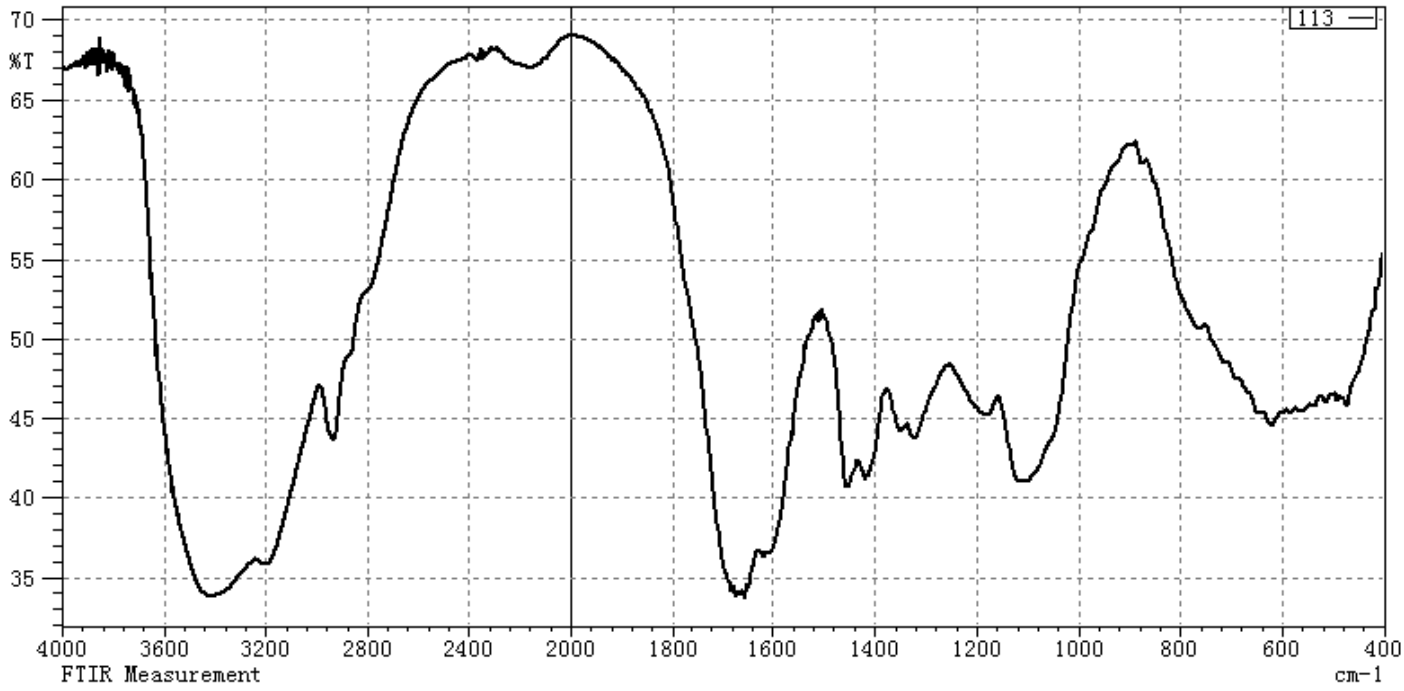

Figure 1

FTIR spectrum of hybrid coal gangue–polyacrylamide

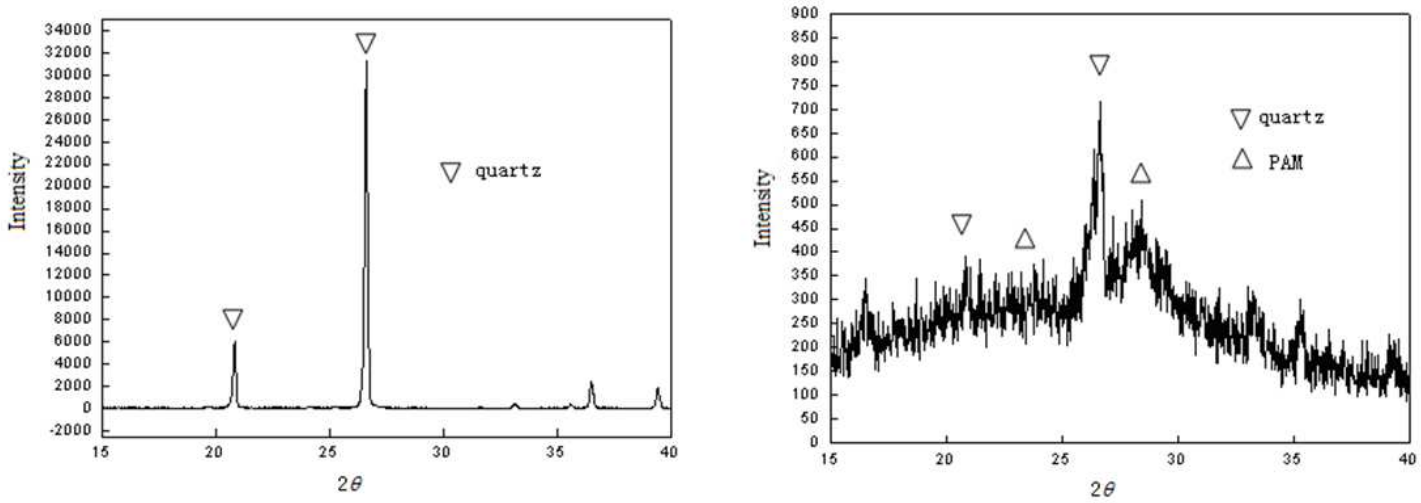

(a) Modified coal gangue **(b)** Hybrid coal gangue–polyacrylamide

Figure 2

XRD patterns of the samples

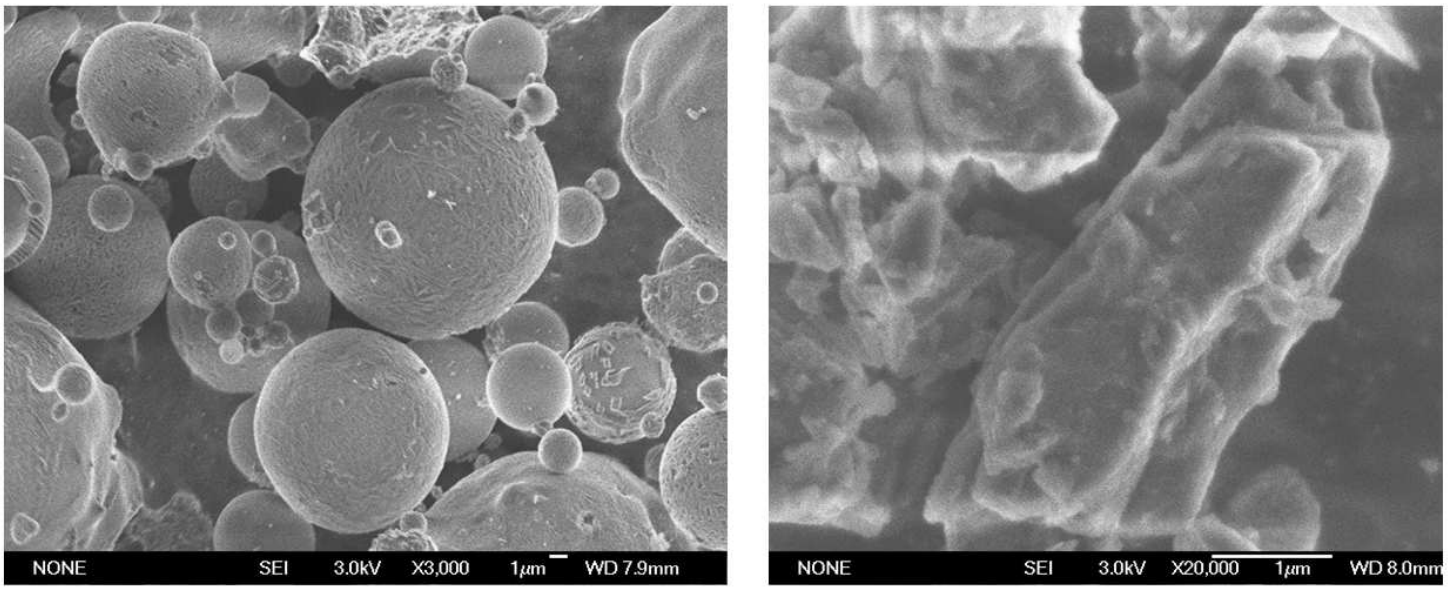

(a) Modified coal gangue (b) Hybrid coal gangue–polyacrylamide

Figure 3

SEM images

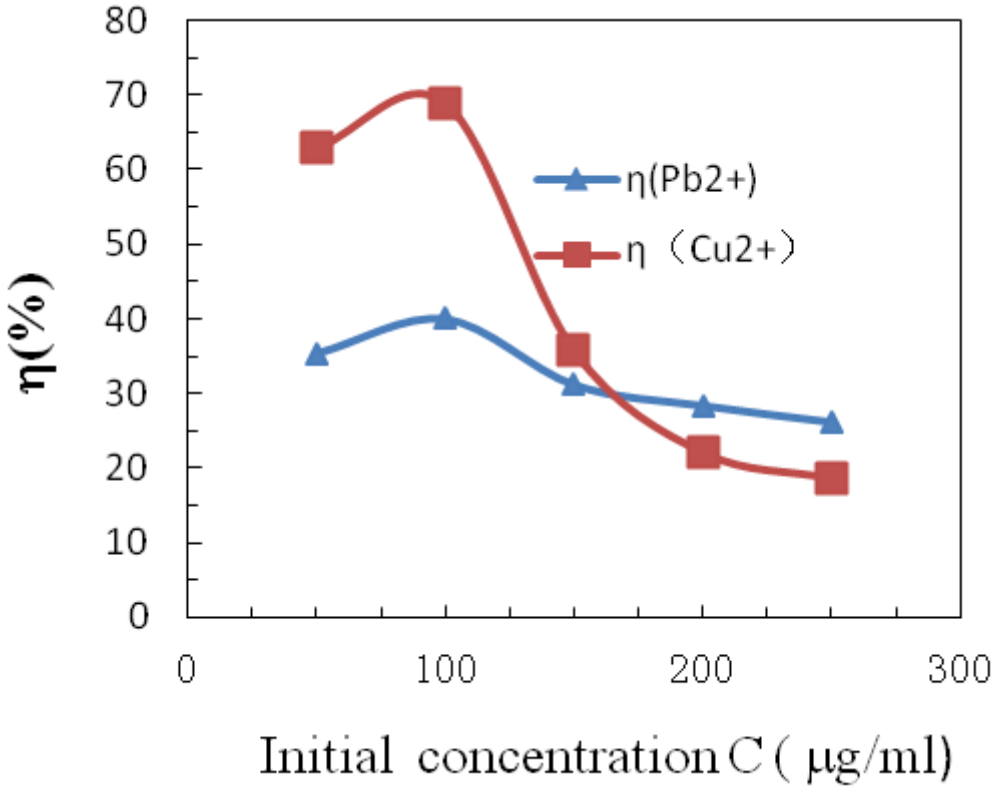

Figure 4

Influencing curve for initial concentration of Pb2+ and Cu2+

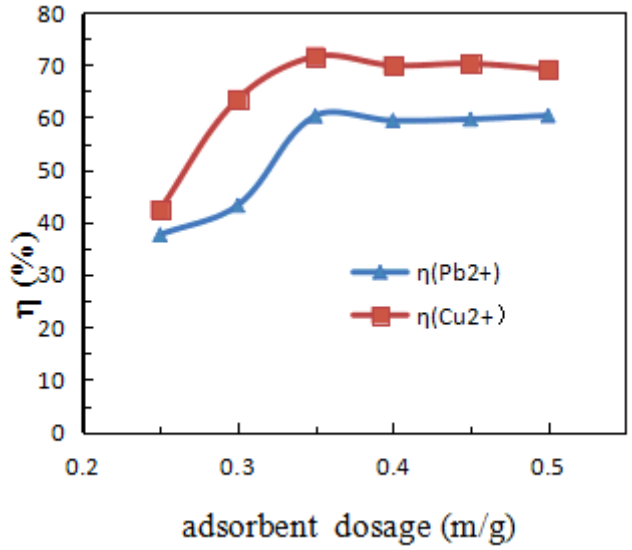

Figure 5

Influence Curve of Adsorbent Dosage of Pb2+, Cu2+

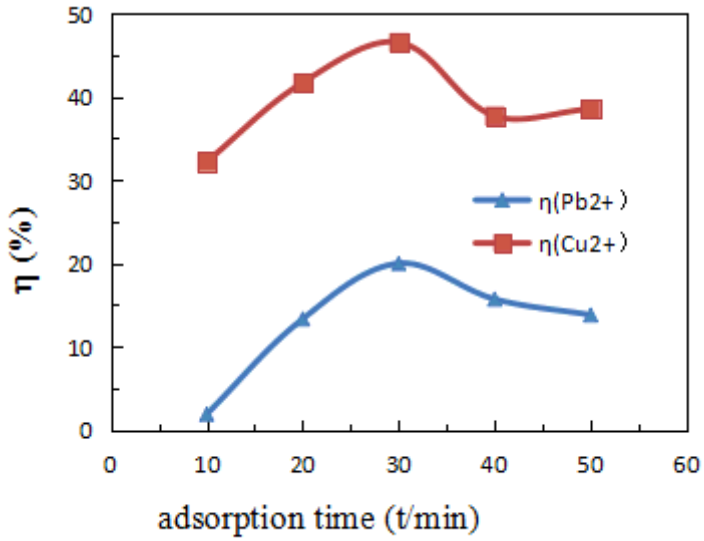

Figure 6

Influence Curve of Adsorption Time of Pb2+, Cu2+

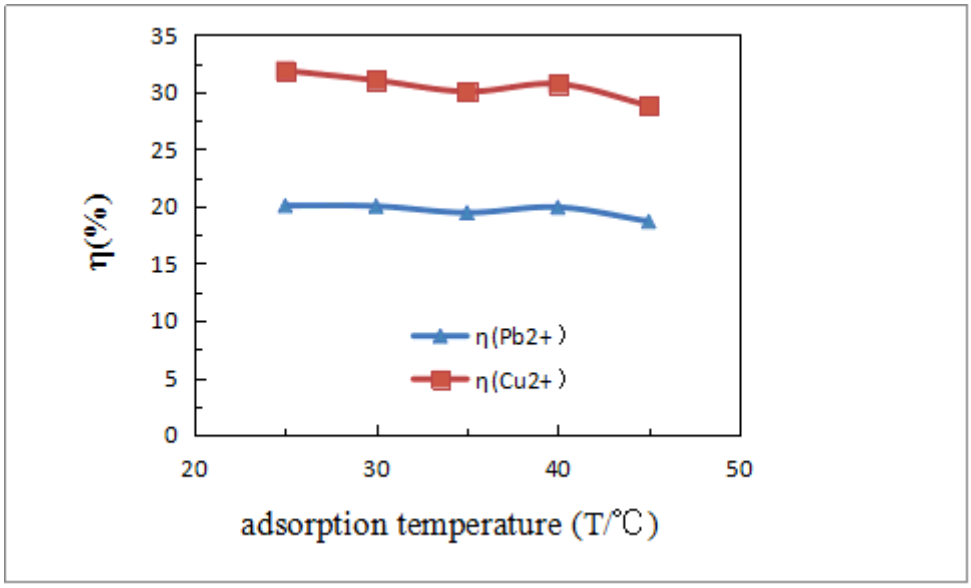

Figure 7

Influence Curve of Adsorption Temperature of Pb2+, Cu2+

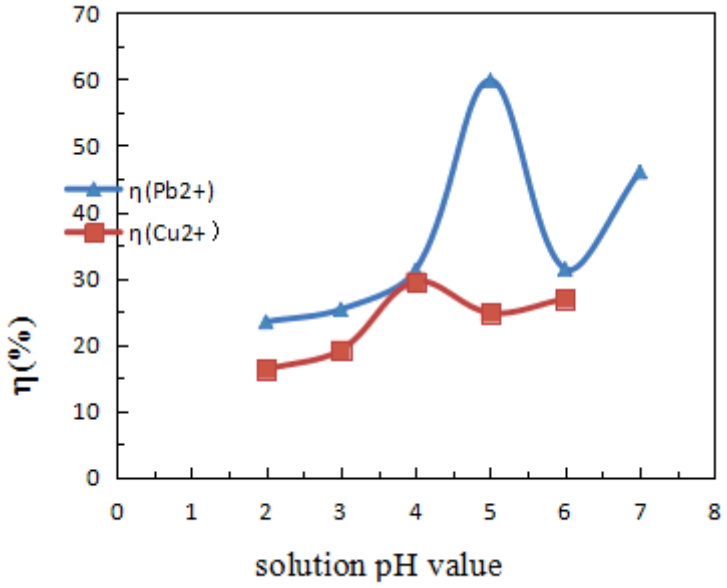

Figure 8

Influence curve of the pH of the Pb2+ and Cu2+ solution

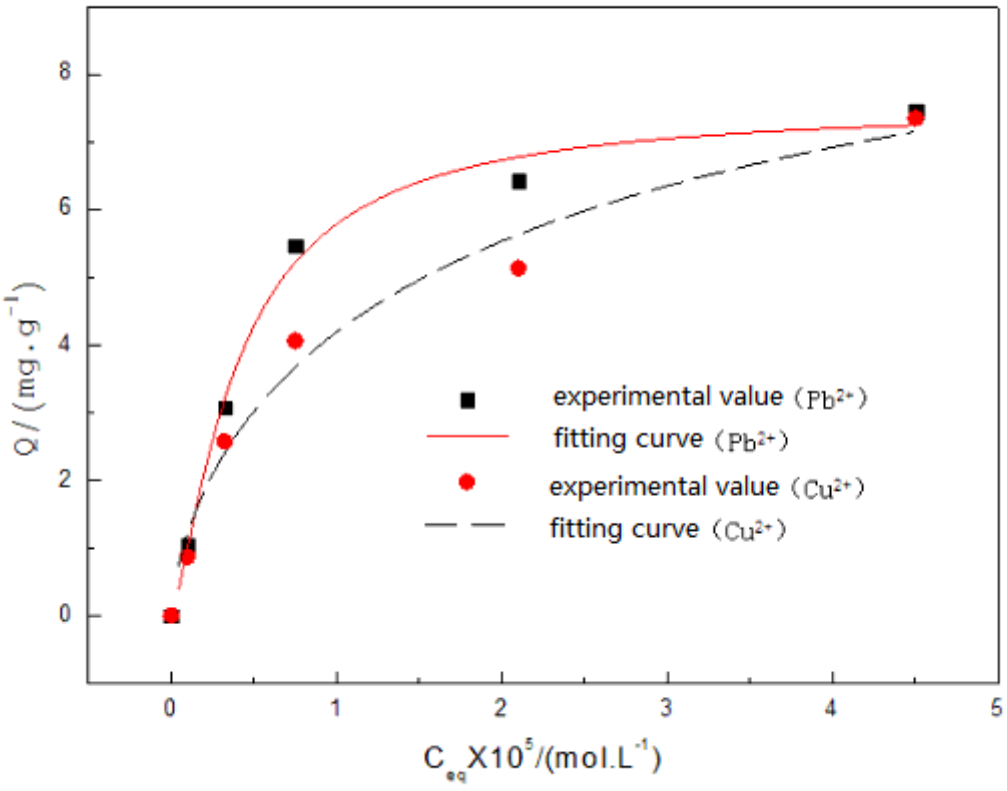

Figure 9

Langmuir model fitting for the adsorption of Pb2+ (Cu2+) onto hybrid coal gangue–polyacrylamide